Received: 24 June 2019 | Revised: 3 November 2019 | Accepted: 5 November 2019

DOI: 10.1002/fsn3.1347

Food Science & Nutrition Open Access WILEY

ORIGINAL RESEARCH

Prediction kinetic, energy and exergy of quince under hot air dryer using ANNs and ANFIS

Yousef Abbaspour-Gilandeh | Ahmad Jahanbakhshi | Mohammad Kaveh

Department of Biosystems Engineering, College of Agriculture and Natural Resources, University of Mohaghegh Ardabili, Ardabil, Iran

Correspondence
Yousef Abbaspour-Gilandeh, Department of Biosystems Engineering, College of Agriculture and Natural Resources, University of Mohaghegh Ardabili, Ardabil, Iran.
Email: abbaspour@uma.ac.ir

Funding information
University of Mohaghegh Ardabili

Abstract

This study aimed to predict the drying kinetics, energy utilization (E_u), energy utilization ratio (*EUR*), exergy loss, and exergy efficiency of quince slice in a hot air (HA) dryer using artificial neural networks and ANFIS. The experiments were performed at air temperatures of 50, 60, and 70°C and air velocities of 0.6, 1.2, and 1.8 m/s. The thermal parameters were determined using thermodynamic relations. Increasing air temperature and air velocity increased the effective moisture diffusivity (D_{eff}), E_u, *EUR*, exergy efficiency, and exergy loss. The value of the D_{eff} was varied from 4.19×10^{-10} to 1.18×10^{-9} m^2/s. The highest value E_u, *EUR*, and exergy loss and exergy efficiency were calculated 0.0694 kJ/s, 0.882, 0.044 kJ/s, and 0.879, respectively. Midilli et al. model, ANNs, and ANFIS model, with a determination coefficient (R^2) of .9992, .9993, and .9997, provided the best performance for predicting the moisture ratio of quince fruit. Also, the ANFIS model, in comparison with the artificial neural networks model, was better able to predict E_u, *EUR*, exergy efficiency, and exergy loss, with R^2 of .9989, .9988, .9986, and .9978, respectively.

KEYWORDS
adaptive neuro-fuzzy inference system, artificial neural networks, drying, quince, thermodynamic parameters

1 | INTRODUCTION

Drying is one of the oldest procedures for preserving food and agricultural products. Drying is defined as the reduction in moisture from the products and is the most important process for preserving agricultural products since it has a significant effect on the quality of the dried products. The principle objective in drying agricultural products is the reduction in the moisture content to a level that allows safe storage over an extended period (Mohammadi, Tabatabaekoloor, & Motevali, 2019). Nevertheless, the high consumption of energy in the food drying industry has made it the most consuming and the most important industrial operation. Therefore, one of the most substantial challenges in dried fruit industry is to reduce the cost of energy sources to produce dry quality products. So, useful thermodynamic analysis of dryers is necessary when we aim to save energy consumption and optimize process variables (Roknul Azam, Zhang, Law, & Mujumdar, 2019; Shende & Datta, 2019).

Energy and exergy analysis is applied to determine energy needed to dry the product and exergy loss at each stage of the process. Exergy is defined as the maximum amount of work, which can be produced by a stream of matter, heat, or work as it comes to equilibrium with a reference environment. In the drying industry, the goal is to use a minimum amount of energy for maximum moisture removal for the desired final conditions of the product. So,

focusing on energy and exergy analysis is very important (Lingayat, Chandramohan, & Raju, 2018; Yogendrasasidhar & Setty, 2018).

Şevik, Aktaş, Dolgun, Arslan, and Tuncer (2019) analyzed the exergy and energy in the process of drying mint and apple slices in a solar and solar-infrared. The results indicated that the loss of exergy and exergy efficiency increases by increasing the air temperature. Exergy efficiency for mint in solar dryer and solar-infrared was 69.35% and 59.07%, respectively. Akpinar, Midilli, and Bicer (2006) analyzed the energy and exergy in pumpkin. They reported that the pumpkin dried within the time range of 5.66–12 hr with a loss of exergy from 0 to 1.165 kJ/s. The maximum exergy of the system input was 2.198 kJ/s. Also, with increased exergy loss, the energy used in the solar dryer increased. Karthikeyan and Murugavelh (2018) studied the energy and exergy required to dry turmeric in a mixed-mode forced convection solar tunnel dryer and concluded that the loss of exergy and energy utilization ratio and its efficiency was increased with increasing temperature.

Recently, several studies have been carried out to energy and exergy analysis in the process of drying products such as potato slices in solar dryer (Kesavan, Arjunan, & Vijayan, 2019), turmeric slices in microwave dryer (Surendhar, Sivasubramanian, Vidhyeswari, & Deepanraj, 2019), Kodo millet grains and fenugreek seeds using wall heated fluidized bed dryer (Yogendrasasidhar & Setty, 2018), dog-rose flowers with a hybrid infrared-hot air dryer (Motevali, Jafari, & Hashemi, 2018), and tomato slices in a solar dryer (Arepally, Ravula, Malik, & Kamidi, 2017).

The base of intelligent methods work is using hidden knowledge in the experimental data, trying to extract the inherent relationships among them and generalizing results to other situations. Artificial neural networks are one of the most essential methods used in the field of artificial intelligence was inspired by how the human brain works, training takes place first, and then the information related to the data is stored in the form of the network's weights (Jahanbakhshi, Ghamari, & Heidarbeigi, 2017; Sun, Zhang, & Mujumdar, 2019). Artificial neural networks and ANFIS have been successful in estimations in natural processes. These methods have advantages over many conventional statistical and deterministic procedures. Compared to linear regression models, they do not necessitate the placement of prediction values around the mean and thus reflect the real data variability (Jahanbakhshi & Salehi, 2019; Kaveh, Jahanbakhshi, Abbaspour-Gilandeh, Taghinezhad, & Moghimi, 2018; Movagharnejad & Nikzad, 2007; Shekarchizadeh, Tikani, & Kadivar, 2014).

Liu et al. (2019) have surveyed ANNs application to predict E_u, *EUR*, exergy loss, and exergy efficiency mushroom slices in HA dryer. The results indicated that value R^2 for E_u, *EUR*, exergy loss, and exergy efficiency was .9978, .985, .994, and .998, respectively. Checking drying index (moisture content (*MC*) and drying rate) and thermodynamic parameters (energy and exergy efficiency) of drying banana in HA flow dryer with the help combined structure ANNs-RSM showed that this structure is able to predict drying index and thermodynamic parameters with $R^2 > .96$ and RMSE < 0.060 (Taheri-Garavand, Karimi, Karimi, Lotfi, & Khoobbakht, 2018). Kaveh, Jahanbakhshi, et al. (2018) tried to predict *MR* of almond fruit in the process of drying in a convective dryer with ultrasound pretreatment through mathematical models, ANNs and ANFIS and reported that to predict moisture ratio in almond, ANFIS model with the R^2 = .9998 and *MSE* = 0.003 had a better performance.

It was founded in a study in which potato slice, energy and exergy in fluidized bed method was modeled with the help of the neural network that can predict energy and exergy of potato slice with best and highest accuracy. In this investigation, drying time, air temperature, inlet airspeed, and depth variables were considered as network inputs (Azadbakht, Aghili, Ziaratban, & Torshizi, 2017).

The detailed literature review for the present study has shown that there is no information on energy and exergy analysis and other parameters of the thin-layer drying process of quince fruit via hot air dryer. Therefore, this paper, as a novel study, concentrates on the energy and exergy analysis of the thin-layer drying of quince fruit via hot air dryer by using the first and second law of thermodynamics. The primary objective of this study is to present modeling, analysis of kinetics, D_{eff}, E_a, *SEC*, energy and exergy analysis of thin-layer drying of quince fruit at different conditions in a hot air dryer. It is believed that such a study will contribute to quince fruit producers by removing their problems related to energy and exergy throughout the drying process.

2 | MATERIALS AND METHODS

2.1 | Preparing the samples

In this research, quince fruits were purchased from a local market in Ardebil, Iran. After being washed, fruits in good shape were selected for the experiment. Samples were stored in a refrigerator at the temperature of 4°C to be prepared and to reach similar initial temperature before the experiments. The initial *MC* of the samples was obtained by using the Memmert standard oven for 24 hr at the temperature of 70°C (Jahanbakhshi, 2018), which was equal to 5.52 ± 0.5% on a dry basis.

2.2 | Hot air dryer

To carry out the experiments, a HA dryer was used. The samples to be tested were placed in the middle of the airflow channel of the dryer in a meshed bowl on a digital scale with a precision of 0.01 g attached below the dryer and situated outside the airflow channel. The laboratory dryer used in this study had a centrifugal blower, which blew HA over the samples in a parallel manner. To begin the experiment, the device was first put on and worked for 15 min so that the dryer would reach balance temperature. Then, the quince samples were placed on the dryer's bed and the weight of the samples was measured in 5-min intervals by a scale (AND, GF-6000) and recorded in a computer.

The relative temperature and moisture in the ambient around the dryer are two determining variables in drying foodstuff. Thus, in each experiment, the relative temperature and moisture around the dryer were measured and recorded using a digital Testo 925 thermometer with the accuracy of ±0.1°C and a Testo 400 moisture meter with the accuracy of ±0.1%.

During the drying experiments, the average ranges for changes in ambient temperature and relative air moisture were 25 ± 4°C and 17 ± 5%, respectively. The experiments were conducted at temperatures (50, 60, and 70°C) and three input air velocities (0.6, 1.2, and 1.8 m/s). The thickness of 3 mm was selected for the samples in this study.

The relative moisture ratio (*MR*) of the quince fruit samples can be obtained through Equation (1) (Jahanbakhshi, Rasooli Sharabiani, Heidarbeigi, Kaveh, & Taghinezhad, 2019; Torki-Harchegani, Ghanbarian, Pirbalouti, & Sadeghi, 2016).

$$MR = \frac{M_t - M_e}{M_b - M_e} \tag{1}$$

2.3 | Modeling

To model the drying process, the relative *MR* of the quinces in different treatments was calculated using Equation (1). After determining the relative *MR* values, the data were fitted using ten mathematical models (Table 1) in MATLAB R2014a software.

One of the most important criteria used for specifying the best model is the coefficient of determination (R^2), and the appropriate fitting can be determined using an index called root mean square error (*RMSE*). The model, which has the highest R^2 and the lowest *RMSE*, will be the best model for treatment. These values can be calculated using Equations 2 and 3 (Amiri Chayjan, Kaveh, & Khayati, 2017).

$$R^2 = 1 - \frac{\sum_{i=1}^{N} (y - y')^2}{\sum_{i=1}^{N} (y - \bar{y})^2} \tag{2}$$

$$RMSE = \sqrt{\frac{1}{N} \sum_{i=1}^{N} (y - y')^2} \tag{3}$$

2.4 | Determination of D_{eff}

Fick's second law is used extensively to describe diffusivity in the process of drying agricultural products (Mohammadi et al., 2019):

$$\frac{\partial M}{\partial t} = D_{eff} \nabla^2 \frac{\partial^2 M}{\partial x^2} \tag{4}$$

The initial and boundary conditions are:

$$M(t=0,x) = M_o; \frac{\partial M}{\partial x}(t,x=0) \text{ and } M\left(t,x=\pm\frac{L}{2}\right) = M_s \tag{5}$$

After extending Equation (5) and maintaining the drying conditions for a long time, Equation (6) can be obtained for determining moisture diffusivity (Koukouch et al., 2017):

$$MR = \frac{M_t - M_e}{M_o - M_e} = \frac{8}{\pi_2} \sum_{n=1}^{\infty} \frac{1}{(2n+1)} \exp\left(\frac{-D_{eff}(2n+1)_2 \pi^2 t}{4L^2}\right) \tag{6}$$

Effective moisture diffusivity coefficient (D_{eff}) is obtained through Equation (7) from the gradient (*K*) of the *Ln* (*MR*) graph over time:

$$K = \left(\frac{D_{eff} \pi^2}{4L^2}\right) \tag{7}$$

2.5 | Determination of E_a

Using the Arrhenius equation, the relationship between temperature and D_{eff} is obtained and activation energy can be calculated (Mohammadi et al., 2019).

$$D_{eff} = D_0 \exp\left(-\frac{E_a}{R_g T_a}\right) \tag{8}$$

By drawing the graph *Ln* (D_{eff}) in front of ($1/T_a$), a line with the gradient K_1 is obtained:

$$K_1 = \left(\frac{E_a}{R_g}\right) \tag{9}$$

2.6 | Determination of *SEC*

The value of energy needed to evaporate a kilogram of water from the product in the drying process is defined as *SEC*. Value of the *SEC* used in an HA dryer is taken from two sources. These energies are (a) heat energy (thermal energy) and (b) blower energy (mechanical energy). The heat generator energy is obtained from Equation (10) (Onwude, Hashim, Abdan, Janius, & Chen, 2019):

$$EU_{ter} = (A_{dc}.V_a.C_{pa}.\rho_a.\Delta T.t) \tag{10}$$

The value of ρ_a can be obtained by Equation (11) (Motevali, Minaei, Banakar, Ghobadian, & Khoshtaghaza, 2014):

$$\rho_a = \frac{101.325}{0.287T} \tag{11}$$

The mechanical energy obtained from the blower is calculated through Equation (12) (Rad, Kaveh, Sharabiani, & Taghinezhad, 2018):

$$EU_{mec} = \Delta P.M_{air}.t \tag{12}$$

The *SEC* of the quince fruit in the HA drying is obtained from Equation (13) (Motevali et al., 2014; Rad et al., 2018):

TABLE 1 Applied models to fit the experimental data

Models	Equations	References
Newton (Lewis)	$MR = \exp(-kt)$	Elmas et al. (2019)
Henderson and Pabis	$MR = a\exp(-kt)$	Torki-Harchegani et al. (2016)
Page	$MR = \exp(-kt^n)$	Khanali and Rafiee (2014)
Logarithmic	$MR = a\exp(-kt) + c$	Arepally et al. (2017)
Two-term	$MR = a\exp(-k_0t) + b\exp(-k_1t)$	Ziaforoughi et al. (2016)
Wang and Singh	$MR = 1 + at + bt^2$	Sahin and Doymaz (2017)
Midilli *et al.*	$MR = a\exp(-kt^n) + bt$	Darıcı and Sen (2015)
Parabolic	$MR = a + bt + ct^2$	Coskun et al. (2017)
Logistic	$MR = a/(1 + b\exp(kt))$	Rad et al. (2018)
Demir et al.	$MR = a\exp(-kt)^n + b$	Kaveh, Jahanbakhshi, et al. (2018)

TABLE 2 Formulas used for determining energy utilization and energy utilization ratio of convective dryer

Equation	Equation number	Reference
$Eu = \dot{m}_{da}(h_{dai} - h_{dao})$	(14)	Nazghelichi et al. (2010)
$\dot{m}_{da} = \rho_a V_a A_{dc}$	(15)	Khanali and Rafiee (2014)
$h_{da} = C_{pda}(T - T_{ref}) + h_{fg}w$	(16)	Nazghelichi, Aghbashlo, Kianmehr, and Omid (2011)
$C_{pda} = 1.004 + 1.88w$	(17)	Azadbakht et al. (2017)
$w = 0.622 \times \frac{\phi \times P_{vs}}{P - P_{vs}}$	(18)	Zohrabi, Seiiedlou, Aghbashlo, Scaar, and Mellmann (2019)
$w_{dao} = w_{dai} + \frac{\dot{m}_v}{\dot{m}_{da}}$	(19)	Azadbakht et al. (2017)
$\dot{m}_v = \frac{w_t - w_{t+\Delta t}}{\Delta t}$	(20)	Khanali and Rafiee (2014)
$EUR = \frac{\dot{m}_{da}(h_{dai} - h_{dao})}{\dot{m}_{da}(h_{dai} - h_{dae})}$	(21)	Nazghelichi et al. (2010)

TABLE 3 Formulas used for determining Exergy loss and Exergy loss of convective dryer

Equation	Equation number	Reference
$\dot{E}x_{dci} = \dot{m}_{da}C_{Pda}\left[(T_{dci} - T_\infty) - T_\infty \ln\frac{T_{dci}}{T_\infty}\right]$	(22)	Zohrabi et al. (2019)
$\dot{E}x_{dco} = \dot{m}_{da}C_{Pda}\left[(T_{dco} - T_\infty) - T_\infty \ln\frac{T_{dco}}{T_\infty}\right]$	(23)	Motevali et al. (2018)
$\dot{E}x_y = \dot{E}x_{dci} - \dot{E}x_{dco}$	(24)	Arepally et al. (2017)
$\eta_{Ex} = \frac{\dot{E}x_{dci} - \dot{E}x_y}{\dot{E}x_{dci}} = 1 - \frac{\dot{E}x_y}{\dot{E}x_{dci}}$	(25)	Liu et al. (2019)

$$SEC = \frac{EU_{(mec+ter)}}{M_W} \quad (13)$$

2.7 | Energy analysis

The energy utilization (E_u), mass flow of air ($\dot{m}_{da}$), dry air enthalpy (h_{da}), specific heat of input and output air (C_{pda}), air humidity ratio (kg water/kg dry air) (w), ratio of air humidity to the inlet and outlet (w_{dao}), mass transfer rate (kg water/s) ($\dot{m}_v$), and energy utilization ratio (*EUR*) calculated through the first law of thermodynamics can be expressed as follows (Table 2):

2.8 | Analysis of exergy

Exergy of air at the entrance to the drying chamber, exergy of air at the outlet of the drying chamber, exergy loss ($\dot{E}\ x_y$), and exergy efficiency (η_{Ex}) obtained using (Equations 21–24) in (Table 3).

2.9 | Artificial neural networks

The network architecture consists of an input layer with three neurons, an output layer and one or two hidden layers (Figure 1). The input layer consists of three variables (air temperature, air velocity, and drying time), and the output layer has one variable (*MR*, E_u, *EUR*, exergy loss, and exergy efficiency) for the quince fruit drying process. It is difficult to determine the optimal number of neurons in the hidden layer, and it usually depends on the type and complexity of the work. Thus, it is determined by trial and error.

For artificial neural networks, single-layer and double-layer cascade Forward Back Propagation (CFBP) and Feed Forward Back Propagation (FFBP) networks were used, with different numbers of neurons varying between 3 and 15. Moreover, the Levenberg-Marquardt (LM) and Bayesian Regularization (BR) algorithms were used. Three threshold functions namely sigmoid activation function (Logsig), linear activation function (Purelin), and hyperbolic tangent activation function (Tansig) were used to predict the proposed parameters (Jahanbakhshi & Salehi, 2019; Savari, Moghaddam, Amiri, Shanbedi, & Ayub, 2017).

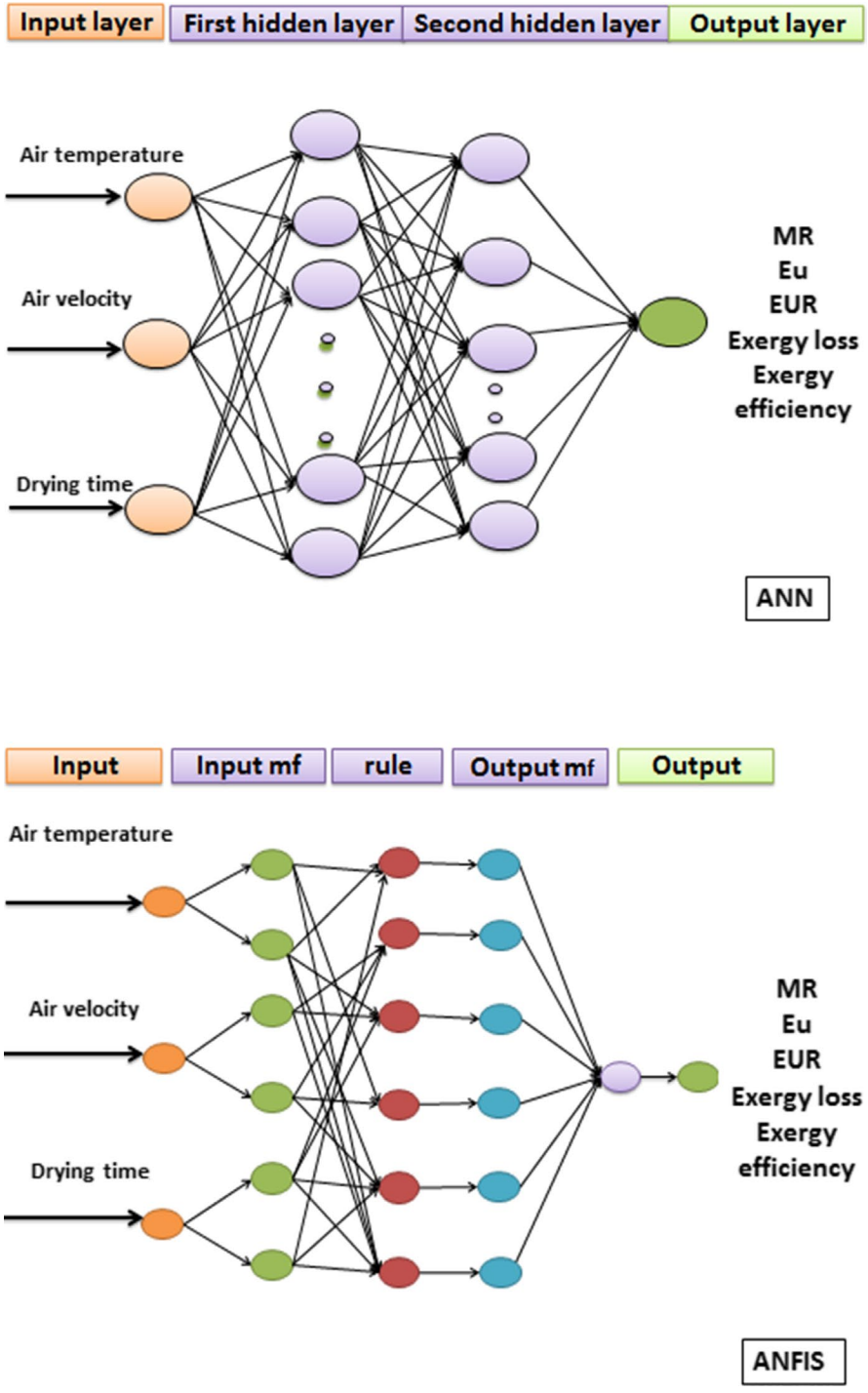

FIGURE 1 ANN and ANFIS structure

2.10 | ANFIS

ANFIS consists of a set of if–then rules and pairs of fuzzy input–output data that use artificial neural networks learning algorithms for training (Al-Mahasneh, Aljarrah, Rababah, & Alu'datt, 2016). ANFIS is very similar to a fuzzy inference system, and the only difference between the two is the use of the backpropagation error algorithm by ANFIS to minimize error. ANFIS's function is very much like those of artificial neural networks and fuzzy logic. In both of these methods, the input passes through the input layer (by the input membership function), and then, the output of the model is obtained in the output layer (by the membership function of the output) (Ziaforoughi, Yousefi, & Razavi, 2016).

Each ANFIS model consists of five layers: (a(Fuzzification, (b(Multiplication, (c(Normalization, (d(Defuzzification, and (e) Summation (Eski et al., 2018) (Figure 1). In the ANFIS analysis, as with other models, the best architecture should be designed. To achieve this objective, ANFIS models are designed using the trial and error method to determine the number of fuzzy rules in output prediction. Eight types of membership functions, namely psigmf, dsigmf, pimf, Gasuss2mf, Gaussmf, gbellmf, trimf, and trapmf can be used as the input to the ANFIS model (Kaveh, Sharabiani, et al., 2018). The number of rules for the membership functions varied from 3 to 5. Moreover, a linear function was selected as the output ANFIS membership function and a hybrid learning method was used.

The present study was modeled using ANNs and ANFIS to predict experimental data on quince fruit drying (*MR*, E_u, *EUR*, exergy loss, and exergy efficiency). Training data and data simulation were conducted in Toolbox of Matlab R2014a software. For network modeling, the data were randomly assigned to two groups, of which 75% were used for training and 25% were applied for testing models.

3 | RESULTS AND DISCUSSION

3.1 | Drying kinetic

After obtaining *MR* at different temperatures and different drying rates, the drying curves were fitted to the experimental data (Figure 2). The results show that the initial *MC* of the product is high and the moisture loss rate is high at the beginning of the drying process (Sahin & Doymaz, 2017). Gradually, as time passes, the initial *MC* of the product decreases naturally over time. The product's drying curve moves downwards at a high gradient at the beginning of the process due to the evaporation of surface moisture, and after this time, due to the onset of water penetration from inside the material to the surface, the curve falls at a lower gradient level (Coskun, Doymaz, Tunçkal, & Erdogan, 2017). At lower velocities, the total drying time is longer. As the temperature rises, the time required for the product to dry decreases due to increased moisture evaporation rate. The effect of temperature on drying time is greater than that of the dryer air velocity in the process of drying the product (Darıcı & Sen, 2015). Moreover, the process of decrease in *MC* under different test conditions shows that increase in air flow rate in the HA dryer reduces the drying time of the product. The reason for this phenomenon is that by increasing air velocity, the vapor pressure of the environment is reduced and, as a result, the *MC* of the product will face less resistance to exit and will be released more quickly (Elmas, Varhan, & Koç, 2019; Kaveh, Sharabiani, et al., 2018). The decreasing of drying time with increasing of drying air temperature and air velocity has been reported for many agricultural products such as jujube slices (Elmas et al., 2019), potato slice, garlic, cantaloupe (Kaveh, Sharabiani, et al., 2018), mushroom slices (Ghanbarian, Dastjerdi, & Torki-Harchegani, 2016), beef (Ahmat, Barka, Aregba, & Bruneau, 2015).

3.2 | Drying model

The values of R^2 and *RMSE* related to the data obtained from the experiments (experimental data) and the data from the models (predicted data) for each of the temperatures and input air velocities are reported in Table 4. Of the ten models, the model with the highest R^2 value and the lowest *RMSE* value was selected as the appropriate model. According to Table 4, the model proposed by Midilli et al. was selected as the best model for describing the quince fruit's drying behavior in a HA dryer with mean R^2 of .9992 and *RMSE* of 9.1×10^{-3}.

3.3 | Effective moisture diffusivity

Figure 3 shows the D_{eff} of the quince fruit at different temperatures and input air velocities. The results show that the D_{eff} increases with increase in drying temperature and air velocity. The D_{eff} varies from 4.19×10^{-10} to 1.18×10^{-9} for temperature range of 50 to 70°C and air velocity of 0.6 to 1.8 m/s. By increasing the temperature of the dryer chamber, the moisture transfer rate from inside the fruit to its surface increases and the D_{eff} increases around three times (Sahin & Doymaz, 2017). In addition, the D_{eff} of quince fruit indicates that the values obtained in this study were within the range of D_{eff} content for foodstuff which is 10^{-12} to 10^{-8} (Kaveh, Jahanbakhshi, et al., 2018). Similar results about the D_{eff} have been reported by other researchers that shown in Table 5.

3.4 | Activation energy

The value of the E_a for the quince fruit in a HA dryer was obtained within the range of 33.06 to 34.77 kJ/mol (Table 6). Therefore, the amounts reported in this study for the E_a of the quince fruit were within the recommended range (12.7 to 110 kJ/mol) for agricultural products (Aral & Bese, 2016; Samimi-Akhijahani & Arabhosseini, 2018).

Value of the E_a represents value of energy required to start mass transfer from the body of the product. If the *MC* is absorbed by the

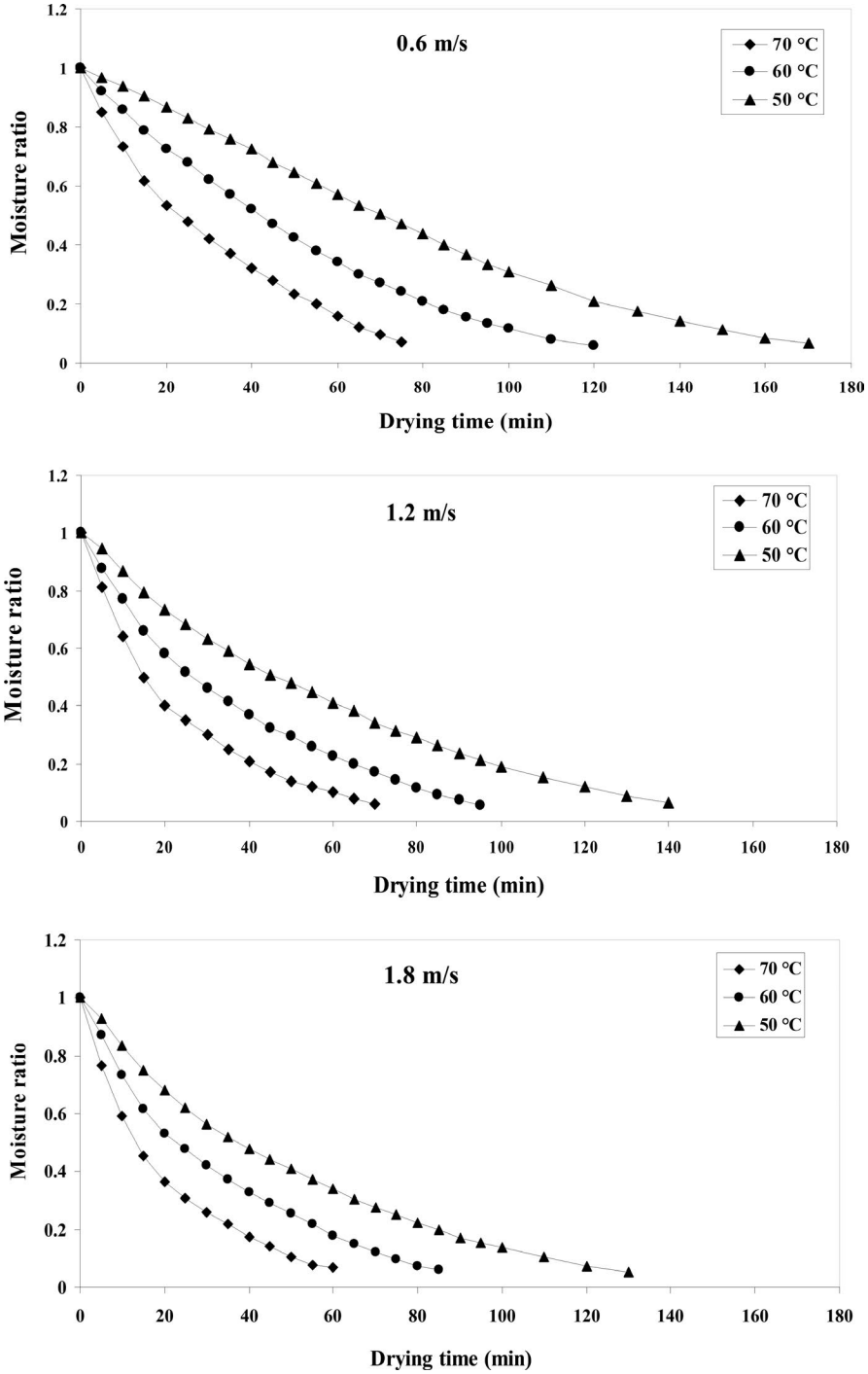

FIGURE 2 Moisture ratio variation in quince fruit under convective drying (air velocity and air temperature)

surface, it requires less energy to start evaporation (Aghbashlo, Kianmehr, & Samimi-Akhijahani, 2008). In similar studies, E_a for hawthorn was obtained between 78.74 and 91.54 kJ/mol (Aral & Bese, 2016) and for tomatoes, it was 12.43 kJ/mol (Coskun et al., 2017).

3.5 | Specific energy consumption

The maximum and minimum amounts of *SEC* by quince fruit were calculated to be between 85.40 and 260.11 kWh/kg (Figure 4). As the temperature of the input air increased, *SEC* decreased due to the significant increase in the drying rate at higher levels of input air temperature. In other words, although by increase in the temperature of the input air, the thermal power applied increases according to Equation 12, due to the reduction in the drying time, thermal energy required to remove the unit of moisture from the product decreased. At low temperatures, drying time and *SEC* amount increase (Motevali et al., 2014).

Motevali and Tabatabaei (2017) have achieved similar results in examining the drying process for dog-rose in a HA dryer. For drying apples in a HA dryer, Majdi, Esfahania, and Mohebbi (2019) obtained an *SEC* amount between 5.5 and 8.9 kWh.

TABLE 4 The statistical comparison for prediction of thin-layer drying of quince

Model	R^2	*RMSE*
Newton (Lewis)	.9970	0.0152
Henderson and Pabis	.9979	0.0122
Page	.9959	0.0182
Logarithmic	.9980	0.0118
Two-term	.9975	0.0137
Wang and Singh	.9966	0.0169
Midilli et al.	**.9992**	**0.0091**
Parabolic	.9985	0.0105
Logestic	.9987	0.0099
Demir et al.	.9947	0.0219

process of drying quince fruit. The maximum of E_u was 0.0694 kJ/s at 70°C and the input air velocity of 1.8 m/s. The minimum amount of E_u was equal to 0.009 kJ/s.

3.6.1 | Effect of air temperature

Figure 5 shows that the E_u increased by an increase in the input air temperature. The highest amount of E_u was observed at the beginning of the drying process and this amount decreased with time. During the drying time, due to the faster transfer of moisture, E_u was higher at the beginning of the drying process. Increasing the temperature of the dryer air led to increase in the input enthalpy and higher heat and mass transfer resulting in higher energy consumption and a higher amount of moisture was taken from the product (Nazghelichi, Kianmehr, & Aghbashlo, 2010). These results are similar to those obtained by Azadbakht et al. (2017) for drying a thin layer of potatoes in a fluidized bed dryer, and Aghbashlo, Kianmehr, and Arabhosseini (2008), for drying potatoes in a semi-industrial continuous dryer.

FIGURE 3 Effect of input air velocity and temperature on effective moisture diffusion coefficient

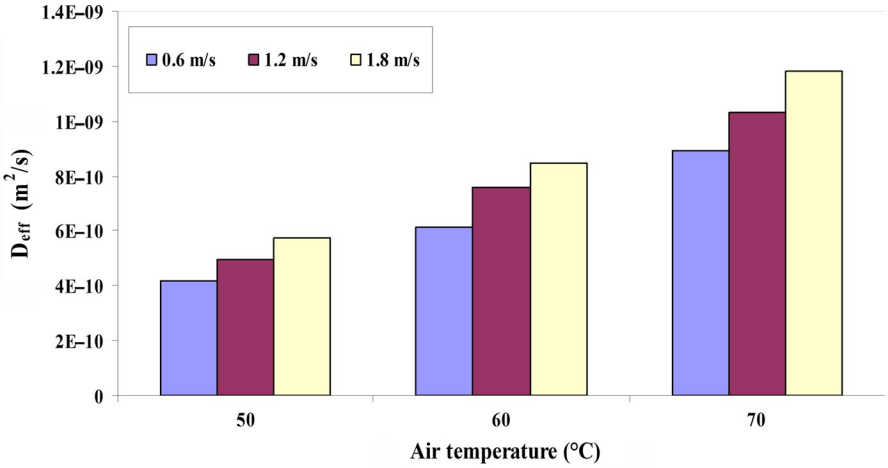

TABLE 5 Effective moisture diffusivity values for some agricultural Products

Fruit	D_{eff}	Reference
Kiwi	$1.94 \times 10^{-9} - 7.12 \times 10^{-9}$ m^2/s	Mohammadi et al. (2019)
Potato	$7.84 \times 10^{-10} - 2.88 \times 10^{-9}$ m^2/s	Boutelba et al. (2019)
Mango cubes	$1.04 \times 10^{-8} - 1.89 \times 10^{-8}$ m^2/s	Sehrawat, Nema, and Kaur (2018)
Olive-tree pruning	$3.41 \times 10^{-8} - 32.5 \times 10^{-8}$ m^2/s	Cuevas et al. (2019)
Walnut	$2.77 \times 10^{-9} - 5.56 \times 10^{-9}$ m^2/s	Abbaspour-Gilandeh, Kaveh, and Jahanbakhshi (2019)

TABLE 6 Activation energy values and related correlation coefficient for quince fruit

Parameter	0.6 m/s	1.2 m/s	1.8 m/s
Activation energy (E_a) (kJ/mol)	34.77	33.71	33.06
Coefficient of determination (R^2)	.9998	.9954	.9991

3.6 | Energy utilization

Energy utilization analysis for the quince fruit was carried out using data from experiments in a hot air dryer. Figure 5 shows the effect of two parameters of temperature and input air velocity on E_u in the

3.6.2 | Effect of air velocity

According to Figure 5, E_u increases with increasing air that enters the drying chamber. Since, the specific energy consumption depends on the velocity of the input air, the hidden heat of water vapor, and the specific heat and the output air temperature, the air mass flow

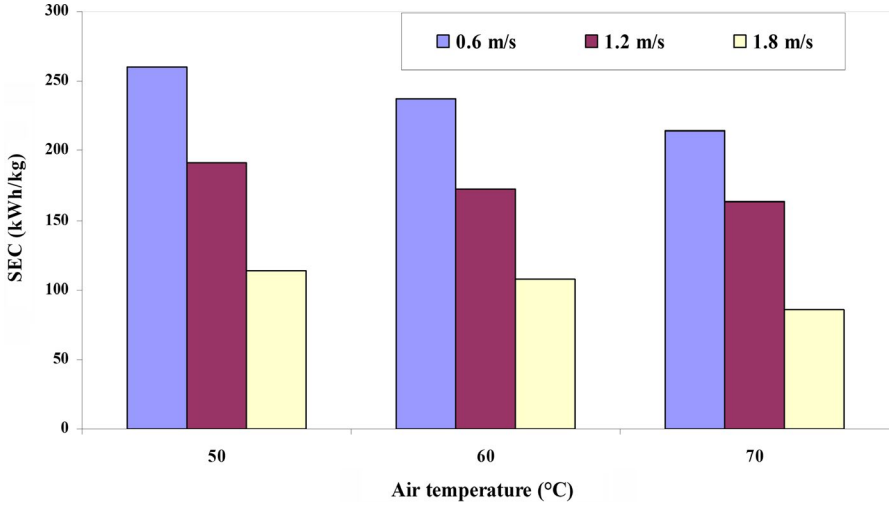

FIGURE 4 Specific energy consumption over temperature and input air velocity

and the enthalpy volume of the input air will increase by increasing airspeed. These conditions will cause the *MC* of the product to evaporate rapidly and increase E_u. These results are consistent with the results of Nazghelichi et al. (2010) regarding drying carrots in the fluidized bed dryer.

3.7 | Energy utilization ratio

Figure 6 shows the *EUR* for the parameters of temperature and air velocity. The highest obtained *EUR* was 0.882 at the temperature of 70°C and airspeed of 1.8 m/s, while the lowest *EUR* was 0.061 at the temperature of 40°C and the airspeed of 0.6 m/s.

3.7.1 | Effect of temperature

The results of Figure 6 show that the *EUR* increases by increasing the temperature of the dryer chamber from 50 to 70°C. The highest *EUR* was observed at the beginning of the drying process, after which *EUR* decreased over time. According to the results, the *EUR* increases with increasing wall temperature in the hot air dryer because increasing the temperature of the dryer chamber increases the heat transfer between the dryer's walls and thus increases the evaporation rate of the *MC* of the product (Darvishi, Azadbakht, & Noralahi, 2018). Aviara, Onuoha, Falola, and Igbeka (2014) showed that in a tray dryer used to dry native cassava starch, *EUR* increased by increasing air temperature. Nikbakht, Motevali, and Minaei (2014) reported the use of hot air with microwave pretreatment for drying pomegranate seeds and concluded that increasing the temperature of the input air would increase the *EUR*.

3.7.2 | Effect of air velocity

The results show that the *EUR* increases by increasing airspeed. Besides, increasing air velocity increases the removal of moisture from the surface of solid material, which in turn would lead to an increase in the *EUR* in the hot air dryer wall (Yogendrasasidhar & Setty, 2018). Yogendrasasidhar and Setty (2018) have studied on energy and exergy analysis of kodo millet grains and fenugreek seeds in fluidized bed dryer and showed that *EUR* increased with increasing air temperature from 40 to 60°C and airspeed from 1.01 to 1.7 m/s.

3.8 | Exergy loss

The effects of two parameters of air temperature and input airspeeds on the exergy loss of drying quince fruits in an HA dryer were studied and its results are shown in Figure 7. The highest exergy loss for drying quince fruits was 0.044 kJ/s at the temperature of 70°C and airspeed of 1.8 m/s, and the lowest exergy loss was 0.0088 kJ/s at the temperature of 50°C and the airspeed of 0.6 m/s.

3.8.1 | Effect of temperature

To calculate the input exergy, the air temperature of the dryer wall is taken into account (Equation 22) and output exergy is determined by the temperature of the output air (Equation 23). The results for exergy loss are shown in Figure 7. According to Figure 7, exergy loss raised by an increase in air temperature. Exergy loss is higher at the initial drying stage and decreases with drying time. In the initial drying phase, exergy loss is high due to the greater evaporation of the product water. This can be attributed to the fact that the difference between the input and output temperature of the drying chamber is high initially and thus more water evaporation from the product takes place (Darvishi et al., 2018). As time passes, the driving force of mass and moisture transfer decreases and the speed of increase in quince fruit exergy decreases over time, which results more significant exergy loss during the process (Corzo, Bracho, Vasquez, & Pereira, 2008).

Aghbashlo, Kianmehr, and Arabhosseini (2008) conducted an exergy loss study on potatoes in a continuous semi-industrial dryer and

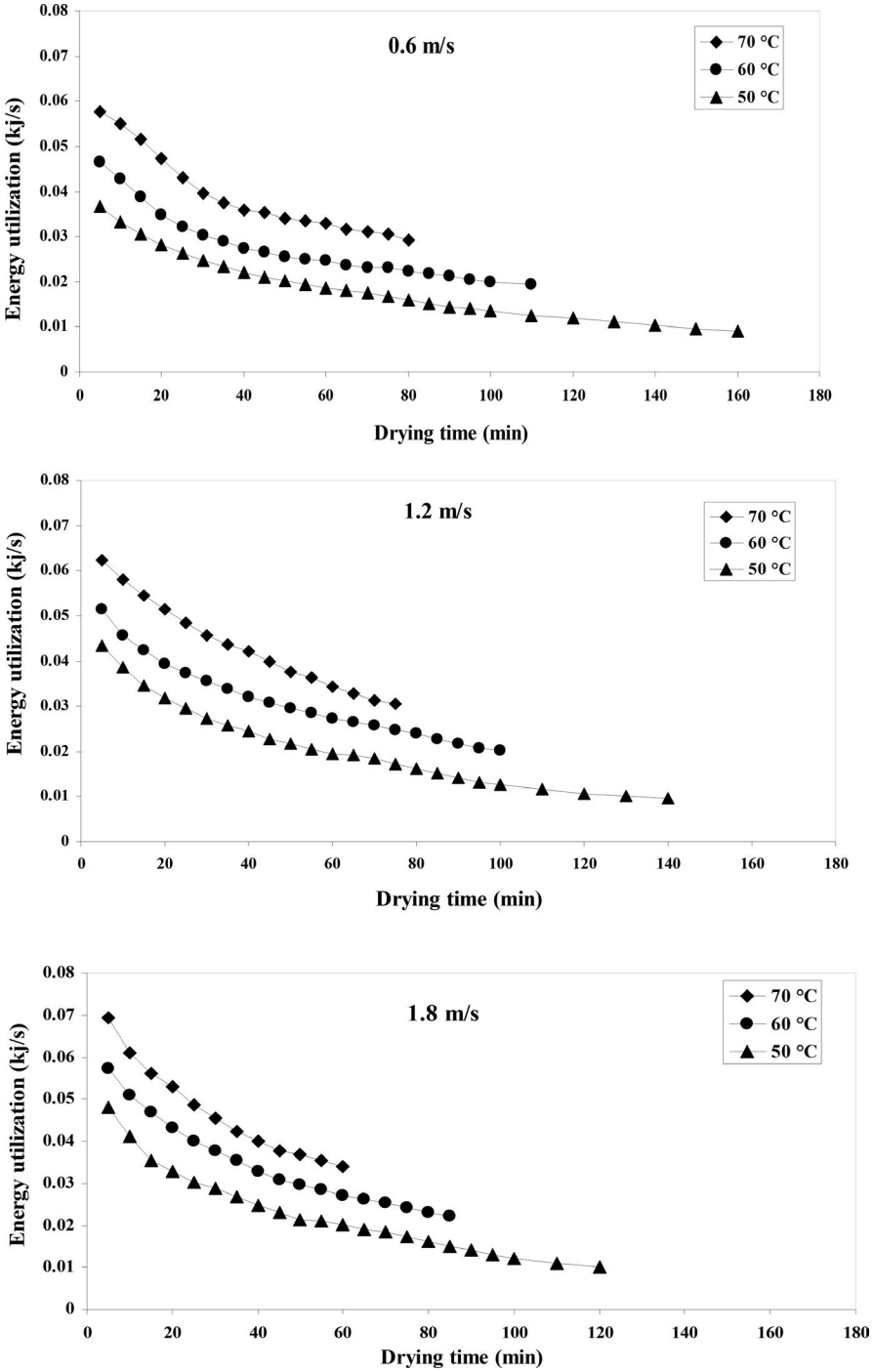

FIGURE 5 Energy utilization variations against drying time at different air temperature and airflow velocities

concluded that exergy loss raised with rising air temperature. The maximum exergy loss was reported to be 13.71 kJ/s at 70°C, and the minimum exergy loss was reported with a rate of 0.5987 kJ/s at 50°C. Colak, Kuzgunkaya, and Hepbasli (2008) reported that exergy loss rises from about 0.09 to about 0.12 kJ/s by increasing air temperature from 40 to 50°C for mint leaves in a tray dryer. In another study by Motevali and Minaei (2012) reported the maximum and minimum exergy loss for pomegranate values of 0.1090 and 0.0336 kJ/s, respectively, for an HA dryer with microwave pretreatment. They also reported that by rising air temperature (from 50 to 70°C), the exergy loss rate increases.

3.8.2 | Effect of air velocity

To determine the exergy loss, the experiments were performed in the velocity range of 0.6 to 1.8 m/s. The results shown in Figure 7 indicate that the exergy loss decreases by rising airspeed due to the high mass propagation force and it also decreases with the passage of the drying time (Azadbakht, Torshizi, Aghili, & Ziaratban, 2018). Nikbakht et al. (2014) have conducted a study on thermodynamic analysis of pomegranate arils in an HA dryer with microwave treatment and reported that exergy loss increased from 0.0235 to 0.1573 kJ/s with increasing airspeed from 0.5 to 1.5 m/s which is

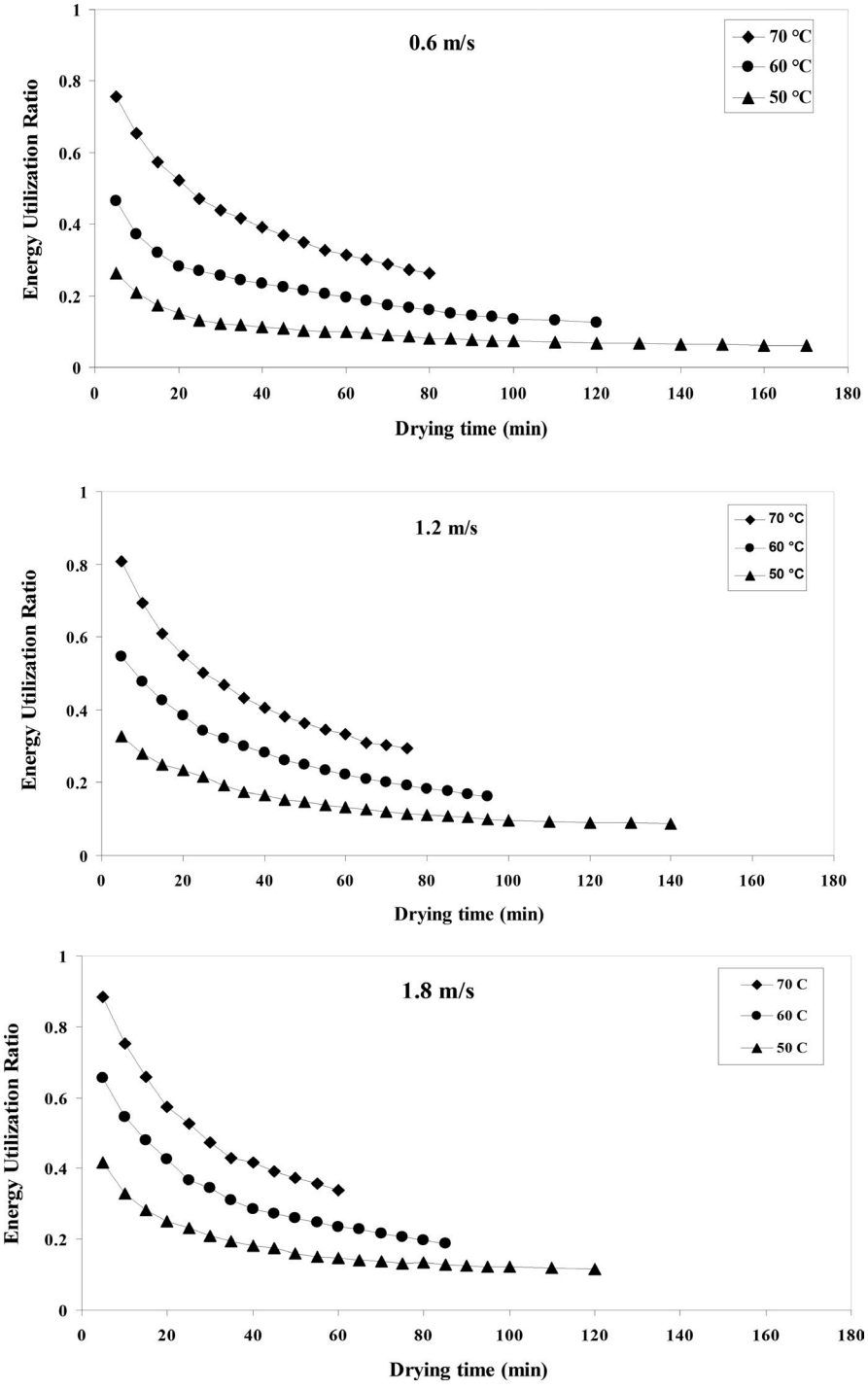

FIGURE 6 Energy utilization ratio variations against drying time at different air temperature and airflow velocities

in agreement with the present study where exergy loss increased (for quince fruit 0.0088 to 0.044 kJ/s) with increase in air velocity Hence, the exergy loss rose by rising the air velocity, being in line with the results of Erbay and Icier (2011) on the olive leaves by exergy analysis in a tray dryer.

3.9 | Exergy efficiency

Exergy efficiency was obtained for quince fruit in the drying experiments at different temperatures and air velocities. The highest amount of exergy efficiency was about 0.879 at the temperature of 70°C and an air velocity of 1.8 m/s. The lowest exergy efficiency was approximately 0.344 at the temperature of 50°C and an air velocity of 0.6 m/s.

3.9.1 | Effect of temperature

Exergy efficiency in an HA dryer within the temperature range of 50 to 70°C is shown in Figure 8. It can be seen that exergy efficiency increases by rising air temperature and drying time.

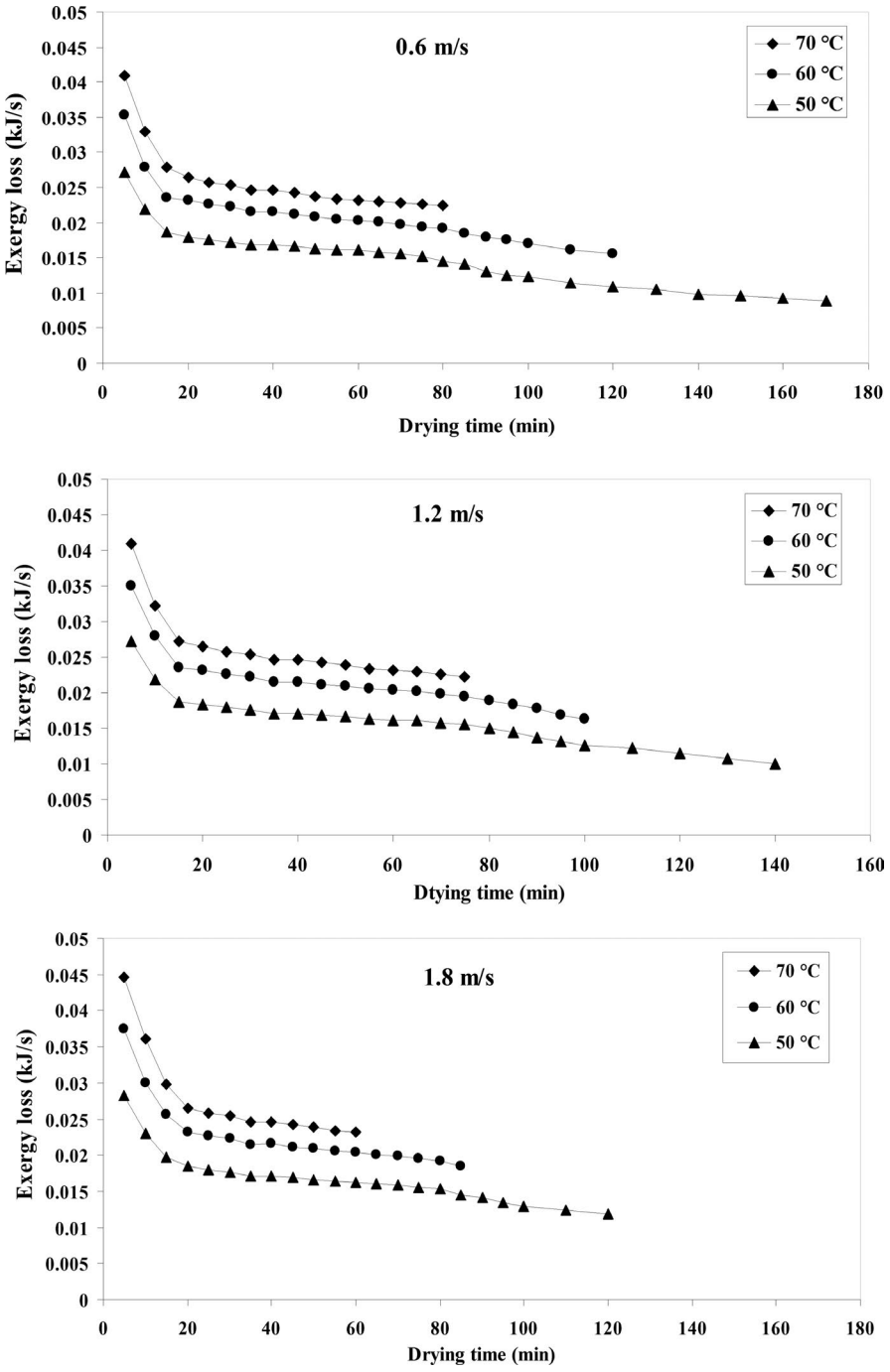

FIGURE 7 Exergy loss (kJ/s) variations against drying time at different air temperature and airflow velocities

Exergy efficiency clearly determines the output exergy of the dryer system in such a way that the output exergy reduces the exergy efficiency due to its high amount of loss in the output air. Exergy loss occurs when the bordering temperature in the dryer is higher than ambient temperature. According to the theory of thermodynamics, exergy efficiency is a proper measure of a drying system (Corzo et al., 2008). These results are similar to what Aktas, Khanlari, Amini, and Sevik (2017) and Ranjbaran and Zare (2013) found about a dryer with infrared-heat pump on carrot and about drying soybeans in microwave-assisted fluidized bed dryer, respectively.

3.9.2 | Effect of air velocity

Exergy efficiency increases by raising the air velocity (Figure 8). This increase in exergy efficiency can be attributed to the high rate of heating and rapid evaporation that takes place in the quince fruit. The entropy and enthalpy of the input air also increase by raising the input air velocity, which results in raised exergy efficiency (Akpinar, Midilli, & Bicer, 2005). In similar studies, researchers reported that exergy efficiency increased by raising the input airspeed (Akpinar et al., 2005; Azadbakht et al., 2017; Yogendrasasidhar & Setty, 2018).

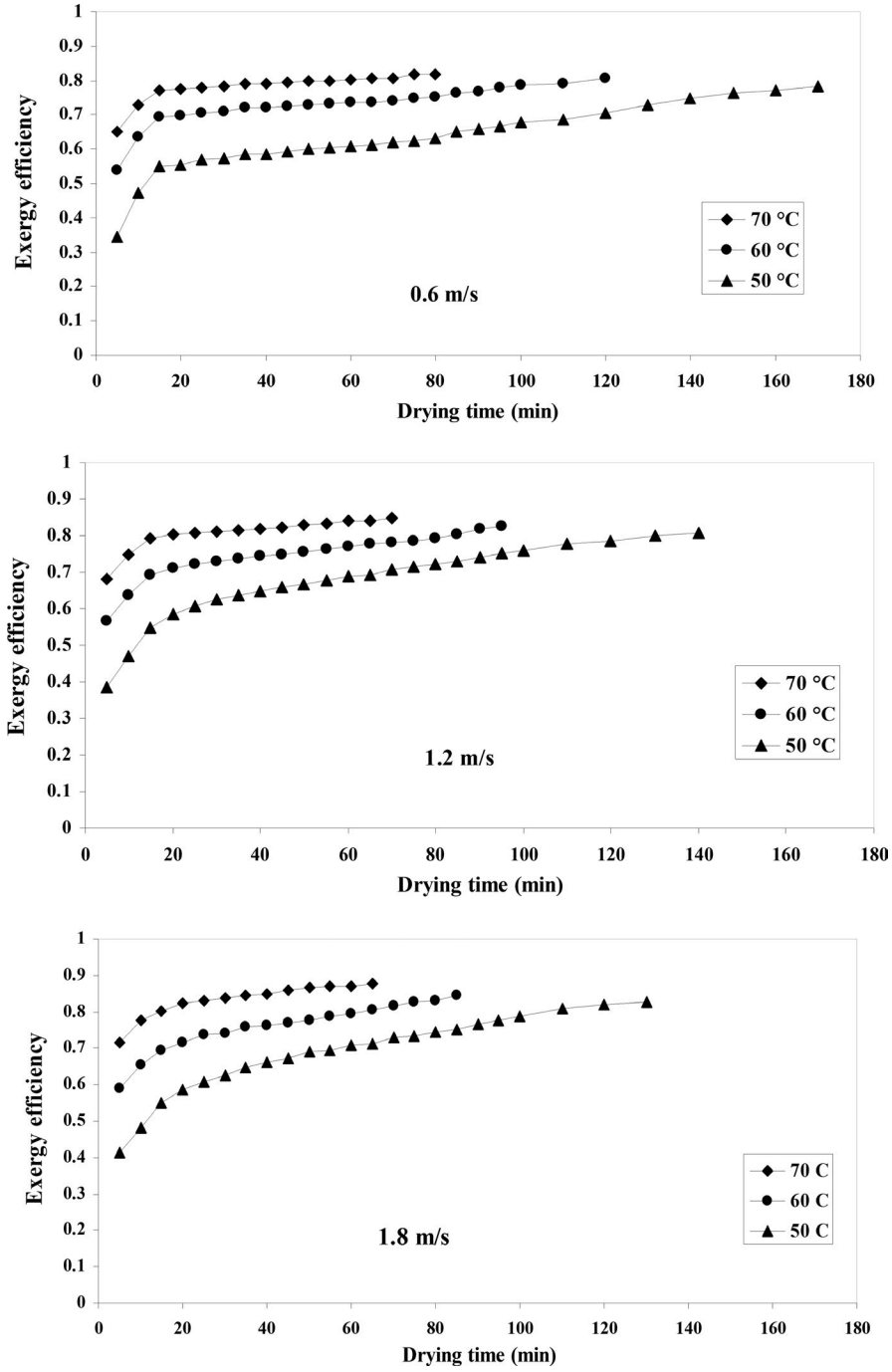

FIGURE 8 Exergy efficiency variations against drying time at different air temperature and airflow velocities

The dryer's thermodynamic efficiency can be improved by the insulation of the drying chamber, designing and choosing the right components, and selecting optimum drying conditions, using other drying techniques such as microwave, infrared, etc. Exergy efficiency is a valuable tool for detecting key system losses and the optimal performance of industrial dryers.

3.10 | Artificial neural networks

In this study, a multilayer perceptron (MLP) was used to predict *MR*, E_u, and *EUR* as well as exergy loss and exergy efficiency. Air velocity, temperature, and drying time were considered as inputs of the network. Moreover, kinetic parameters of drying, E_u, and *EUR* as well as exergy loss and exergy efficiency were selected as network output. The training of the network was based on the two algorithms of BR and LM. Before data entering to the network, they were normalized between 0 and 1.

3.10.1 | Statistical analysis using neural network

The results of modeling artificial neural networks for predicting (a) *MR*, (b) E_u, (c) *EUR*, (d) exergy loss, and (e) exergy efficiency are reported in Table 7.

TABLE 7 ANN result for *MR*, E_u, *EUR*, exergy loss, and exergy efficiency

Parameter	Network	Training algorithm	Threshold function	Number of layers and neurons	*RMSE*	R^2	Epochs
Moisture ratio (*MR*)	FFBP	LM	tansig- tansig- tansig	3-12-12-1	0.0016	.9993	122
Energy utilization (Eu)	FFBP	LM	tansig-logsig- tansig	3-10-10-1	0.0037	.9985	97
Energy utilization ratio (EUR)	FFBP	LM	tansig-logsig-purlin	3-20-15-1	0.0029	.9977	65
Exergy loss	CFBP	BR	tansig-tansig-tansig	3-8-8-1	0.0032	.9980	142
Exergy efficiency	FFBP	LM	tansig-logsig-logsig	3-10-10-1	0.0047	.9970	115

1) To predict the *MR* of the FFBP network, with the topology 3-12-12-1, the tansig–tansig–tansig transfer functions and the LM training algorithm with R^2 = .9993 and *RMSE* = 0.0016, had the best performance. The results indicate that the ANNs modeling technique can be used effectively to predict *MR*. Similar results have been reported by other researchers for other products such as almond (Kaveh, Jahanbakhshi, et al., 2018), onion (Jafari, Ganje, Dehnad, & Ghanbari, 2016), and mushroom (Omari, Behroozi-Khazaei, & Sharifian, 2018).

2) ANNs modeling results for predicting E_u during the process of drying quince fruits are given in Table 7. Given the estimated value of *RMSE* = 0.0037 and R^2 = .9985, the best FFBP network has a topology of 3-10-10-1, with the tansig–logsig–tansig transfer functions and LM training algorithm. Similar results have been reported to predict E_u by other authors including Nikbakht et al. (2014) for pomegranate arils and Azadbakht et al. (2017) for potato cubes using artificial neural networks.

3) According to Table 4, the FFBP network, with 20 neurons in the first hidden layer and 15 neurons in the second hidden layer, with the tansig–logsig–purlin transfer function, as well as the LM algorithm, had the best performance in predicting the *EUR*. In addition, in this network, *RMSE* = 0.0029 and R^2 = .9977. Nikbakht et al. (2014) used ANNs to predict the *EUR*. They obtained a value of R^2 = .9680.

4) The CFBP network with BR algorithm, the tansig–tansig–tansig transfer function, with eight neurons in the first and second hidden layers, and *RMSE* = 0.0032 and R^2 = .9980, had the best prediction for exergy loss.

5) The results of ANNs prediction for exergy efficiency in drying quince fruit in a HA dryer showed that the FFBP network, with a topology 3-10-10-1, the transfer function of tansig–logsig–logsig and the LM training algorithm with *RMSE* = 0.0047 and R^2 = .9970, was selected as the best network. Taheri-Garavand et al. (2018) used ANNs to predict exergy efficiency in drying banana slices in a forced convective dryer. They reported a value of R^2 = .9902. Aghbashlo, Mobli, Rafiee, and Madadlou (2012) also predicted exergy efficiency using artificial neural networks for fish oil and skim milk powder. They obtained R^2 = .9994 and *MSE* = 7.79×10^{-5}.

3.11 | ANFIS

Some changes are required in order to find the best ANFIS network for predicting *MR*, E_u, *EUR*, exergy loss, and exergy efficiency. These changes include the type of membership function, the number of membership functions, and the number of cycles.

The best results for predicting the parameters in question are shown in Table 8. The best MF to predict each of the five parameters after the various changes in the type of membership function was gaussmf membership function. The number of the MFs was determined by the number of the inputs of each ANFIS model.

According to Table 2, R^2 for *MR*, E_u, *EUR*, exergy loss, and exergy efficiency was .9997, .9989, .9988, .9986, .9978, respectively. Also, the values *RSME* for *MR*, E_u, *EUR*, exergy loss, and exergy efficiency were 0.0011, 0.0028, 0.0022, 0.0030, and 0.0046, respectively.

3.12 | Comparison between ANNs and ANFIS model

Comparison of statistical parameters between ANFIS and ANNs models confirms that the ANFIS model has a more accurate performance for predicting each of the five parameters (*MR*, E_u, *EUR*, exergy loss, and exergy efficiency). According to Tables 7 and 8, it

TABLE 8 ANFIS result for *MR*, E_u, *EUR*, exergy loss, and exergy efficiency

	Type of MF		Number of MF				
Parameters	Input	Output	Input	Cycle	Learning method	*RMSE*	R^2
Moisture ratio (*MR*)	Gaussmf	Linear	3-3-3	1,200	Hybrid	0.0011	.9997
Energy utilization (Eu)	Gaussmf	Linear	3-3-3	1,200	Hybrid	0.0028	.9989
Energy utilization ratio (*EUR*)	Gaussmf	Linear	3-5-3	1,200	Hybrid	0.0022	.9988
Exergy loss	Gaussmf	Linear	3-3-3	1,200	Hybrid	0.0030	.9986
Exergy efficiency	Gaussmf	Linear	3-5-3	1,200	Hybrid	0.0046	.9978

can be seen that the value of R^2 for each of the five parameters predicted in the ANFIS model was higher than the artificial neural networks model. Moreover, the value for the ANFIS in all the predicted parameters was lower than the artificial neural networks model.

Khoshnevisan, Rafiee, Omid, and Mousazadeh (2014) used artificial neural networks and ANFIS models to predict the performance of potatoes. They reported that the ANFIS model performed better than the artificial neural network model with respect to its higher R^2 and lower *MSE*. Kaveh, Sharabiani, et al. (2018) predicted four parameters (D_{eff}, *SEC*, *MR*, and *DR*) in drying potato, garlic, and cantaloupe using HA dryers. The ANFIS model showed a higher ability to predict these parameters than artificial neural networks.

4 | CONCLUSIONS

In this research, the effect of temperature and air velocity on drying time, D_{eff}, *SEC*, E_u, *EUR*, exergy loss, and exergy efficiency was investigated. The results of the research showed that among the experimental models, the model of Midilli et al. to describe the kinetics of drying the thin layer of quince fruit slices can be introduced as the most suitable model. The range of D_{eff} in quince fruit samples varied from 4.19×10^{-10} to 1.18×10^{-9} m^2/s, regardless of shrinkage, in the range of temperatures and velocities studied. The highest value of D_{eff} was obtained at the highest levels of temperature and inlet air velocity. With increasing air temperature and air velocity, specific energy consumption, energy utilization, energy utilization ratio, exergy loss, and exergy efficiency increased. The highest E_u and *EUR* were 0.0694 and 0.882 kJ/s at 70°C, respectively. The lowest E_u and *EUR* were 0.009 and 0.061 kJ/s at 50°C, respectively. The highest exergy losses and exergy efficiencies were calculated as 0.044 and 0.879 kJ/s, respectively. Also, the lowest exergy losses and exergy efficiencies were calculated as 0.0088 and 0.344 kJ/s, respectively. ANFIS was one of the fastest methods compared to artificial neural networks with lower *RMSE* and higher R^2 for estimating *MR*, E_u, *EUR*, exergy loss, and exergy efficiency for quince fruit. By insulating the drying chamber, designing and selecting the right components, as well as selecting the optimum drying conditions, the thermodynamic efficiency of the hot air dryer can be increased. Exergy efficiency is a valuable tool for identifying key system losses and optimizing the performance of hot air dryers.

ACKNOWLEDGMENTS

This work was supported by the University of Mohaghegh Ardabili (Contract No. 19502, 97-10-9).

NOMENCLATURE

A_{dc}	Surface area drying chamber (m^2)
C_{pa}	Specific heat (kJ/kg C)
C_{pda}	Specific heat of inlet and outlet air
Eu	Energy utilization (kJ/s)
EUR	Energy utilization ratio (dimensionless)
EU_{mec}	Mechanical energy consumption (Kwh/kg)
EU_{ter}	Thermal energy consumption (Kwh/kg)
E_a	Activation energy (kJ/mol)
$\dot{E}x_{dci}$	Exergy inlet air (kJ/s)
$\dot{E}x_{dco}$	Exergy outlet air (kJ/s)
$\dot{E}x_y$	Exergy loss (kJ/s)
D_0	Width from the source, which is a constant value
D_{eff}	Effective moisture diffusivity coefficient (m^2/s)
L	Half of the thickness of each sample
M_w	Weight loss in the samples (kg)
h_{fg}	Latent heat of vaporization of water (kJ/kg)
h_{da}	Specific enthalpy drying air (kJ/kg)
h_{dai}	Specific enthalpy of inlet air (kJ/kg dryair)
h_{dao}	Specific enthalpy of outlet air
h_{dae}	Specific enthalpy of air environment (kJ/kg dry air)
C_{pda}	Specific heat drying air (kJ/kg K)
$\dot{m}_v$	Mass transfer rate (kg water/s)
$\dot{m}_{da}$	Mass flow rate of drying air (kg/s)
MR	Moisture ratio
M_e	Equilibrium moisture content (% d.b.)
M_t	Moisture content (% d.b.)
M_b	Initial moisture content (% d.b.)
n	index of a summation and the number of terms taken into consideration
N	Number of observations
P	Atmospheric pressure (kPa)
P_{vs}	Saturated pressure (kPa)
R^2	Correlation coefficient
RMSE	Root Mean Square Error
R_g	Universal gas constant equal to 8.3143 kJ/mol
SEC	Specific energy consumption (kWh/kg)
t	Drying time
T_a	Air temperature inside the drying chamber (K)
T_{ref}	Refers to characteristic value
T	Temperature (K)
T_{dci}	Inlet air temperature of drying chamber (K)
T_{dco}	Outlet air temperature of drying chamber (K)
T_∞	Temperature of outlet air (°C)
Va	Input air velocity (m/s)
$w_{t+\Delta t}$	Weight of product at time t + t (kg)
w	Humidity ratio of air (kg water/kg drying air)
w_t	Weight of product at time *t* and
w_{dao}	Outlet humidity ratio of air (kg water/kg drying air
w_{dai}	Inlet humidity ratio of air (kg water/kg drying air)
y	Stands for the experimental values
y′	Predicted values by calculating from the model for this measurements
$\tilde{y}$	The average predicted values
Δt	Time between two sample weighing (s)
ϕ	Relative humidity of air
ρ_a	Air density (kg/m^3)
ΔP	Pressure difference (mbar)
Δt	Temperature difference (°C)
η_{Ex}	exergy efficiency

CONFLICT OF INTEREST

The authors have declared no conflict of interest.

ETHICAL APPROVAL

This study does not involve any human or animal testing.

ORCID

Yousef Abbaspour-Gilandeh https://orcid.org/0000-0002-9999-7845
Ahmad Jahanbakhshi https://orcid.org/0000-0003-1944-3090
Mohammad Kaveh https://orcid.org/0000-0001-5285-2211

REFERENCES

Abbaspour-Gilandeh, Y., Kaveh, M., & Jahanbakhshi, A. (2019). The effect of microwave and convective dryer with ultrasound pre-treatment on drying and quality properties of walnut kernel. *Journal of Food Processing and Preservation*, *43*(11), e14178. https://doi.org/10.1111/jfpp.14178

Aghbashlo, M., Kianmehr, M. H., & Arabhosseini, A. (2008). Energy and exergy analyses of thin-layer drying of potato slices in a semi-industrial continuous band dryer. *Drying Technology*, *26*, 1501–1508. https://doi.org/10.1080/07373930802412231

Aghbashlo, M., Kianmehr, M. H., & Samimi-Akhijahani, H. (2008). Influence of drying conditions on the effective moisture diffusivity, energy of activation and energy consumption during the thin-layer drying of berberis fruit (Berberidaceae). *Energy Conversion and Management*, *49*, 2865–2871. https://doi.org/10.1016/j.enconman.2008.03.009

Aghbashlo, M., Mobli, H., Rafiee, S., & Madadlou, A. (2012). The use of artificial neural network to predict exergetic performance of spray drying process: A preliminary study. *Computer and Electronics in Agriculture*, *88*, 32–43. https://doi.org/10.1016/j.compag.2012.06.007

Ahmat, T., Barka, M., Aregba, A. W., & Bruneau, D. (2015). Convective drying kinetics of fresh beef: An experimental and modeling approach. *Journal of Food Processing and Preservation*, *39*, 2581–2595. https://doi.org/10.1111/jfpp.12508

Akpinar, E. K., Midilli, A., & Bicer, Y. (2005). Energy and exergy of potato drying processvia cyclone type dryer. *Energy Conversion and Management*, *46*, 2530–2552.

Akpinar, E. K., Midilli, A., & Bicer, Y. (2006). The first and second law analyses of thermodynamic of pumpkin drying process. *Journal of Food Engineering*, *72*, 320–331. https://doi.org/10.1016/j.jfoodeng.2004.12.011

Aktas, M., Khanlari, A., Amini, A., & Sevik, S. (2017). Performance analysis of heat pump and infrared–heat pump drying of grated carrot using energy-exergy methodology. *Energy Conversion and Management*, *13*, 327–338. https://doi.org/10.1016/j.enconman.2016.11.027

Al-Mahasneh, M., Aljarrah, M., Rababah, T., & Alu'datt, M. (2016). Application of hybrid neural fuzzy system (ANFIS) in food processing and technology. *Food Engineering Reviews*, *8*, 351–366. https://doi.org/10.1007/s12393-016-9141-7

Amiri Chayjan, A., Kaveh, M., & Khayati, S. (2017). Modeling some thermal and physical characteristics of terebinth fruit under semi industrial continuous drying. *Journal of Food Measurement and Characterization*, *11*, 12–23. https://doi.org/10.1007/s11694-016-9366-4

Aral, S., & Bese, A. V. (2016). Convective drying of hawthorn fruit (Crataegus spp.): Effect of experimental parameters on drying kinetics, color, shrinkage, and rehydration capacity. *Food Chemistry*, *210*, 577–584. https://doi.org/10.1016/j.foodchem.2016.04.128

Arepally, D., Ravula, S. R., Malik, G. K., & Kamidi, V. R. (2017). Mathematical modelling, energy and exergy analysis of tomato slices in a mixed mode natural convection solar dryer. *Chemical Science International Journal*, *20*, 1–11. https://doi.org/10.9734/CSJI/2017/34878

Aviara, N. A., Onuoha, L. N., Falola, O. E., & Igbeka, J. C. (2014). Energy and exergy analyses of native cassava starch drying in a tray dryer. *Energy*, *73*, 809–817. https://doi.org/10.1016/j.energy.2014.06.087

Azadbakht, M., Aghili, H., Ziaratban, A., & Torshizi, M. V. (2017). Application of artificial neural network method to exergy and energy analyses of fluidized bed dryer for potato cubes. *Energy*, *120*, 947–958. https://doi.org/10.1016/j.energy.2016.12.006

Azadbakht, M., Torshizi, M. V., Aghili, H., & Ziaratban, A. (2018). Thermodynamic analysis of drying potato cubes in a fluidized bed dryer. *Carpathian Journal of Food Science and Technology*, *l9*, 167–177.

Boutelba, I., Zid, S., Glouannec, P., Youcef-ali, S., Magueresse, A., & Kimouche, N. (2019). Thermo-hydrous behavior of dried un-blanched potato samples. *Journal of Food Engineering*, *240*, 160–170. https://doi.org/10.1016/j.jfoodeng.2018.07.027

Colak, N., Kuzgunkaya, E., & Hepbasli, A. (2008). Exergetic assessment of drying of mint leaves in a heat pump dryer. *Journal of Food Processing and Engineering*, *31*, 281–298. https://doi.org/10.1111/j.1745-4530.2007.00155.x

Corzo, O., Bracho, N., Vasquez, A., & Pereira, A. (2008). Energy and exergy nalyses of thin layer drying of coroba slices. *Journal of Food Engineering*, *6*, 151–161.

Coskun, S., Doymaz, I., Tunçkal, C., & Erdogan, S. (2017). Investigation of drying kinetics of tomato slices dried by using a closed loop heat pump dryer. *Heat and Mass Transfer*, *53*, 1863–1871.

Cuevas, M., Martínez-Cartas, M. L., Pérez-Villarejo, L., Hernández, L., García-Martín, J. F., & Sánchez, S. (2019). Drying kinetics and effective water diffusivities in olive stone and olive-tree pruning. *Renewable Energy*, *132*, 911–920. https://doi.org/10.1016/j.renene.2018.08.053

Darıcı, S., & Sen, S. (2015). Experimental investigation of convective drying kinetics of kiwi under different conditions. *Heat and Mass Transfer*, *51*, 1167–1176. https://doi.org/10.1007/s00231-014-1487-x

Darvishi, H., Azadbakht, M., & Noralahi, B. (2018). Experimental performance of mushroom fluidized-bed drying: Effect of osmotic pretreatment and air recirculation. *Renewable Energy*, *120*, 201–208. https://doi.org/10.1016/j.renene.2017.12.068

Elmas, F., Varhan, E., & Koç, M. (2019). Drying characteristics of jujube (Zizyphus jujuba) slices in a hot air dryer and physicochemical properties of jujube powder. *Journal of Food Measurement and Characterization*, *13*, 70–86. https://doi.org/10.1007/s11694-018-9920-3

Erbay, Z., & Icier, F. (2011). Energy and exergy analyses on drying of olive leaves (Olea Europaea L.) in tray drier. *Journal of Food Process Engineering*, *34*, 2105–2123. https://doi.org/10.1111/j.1745-4530.2009.00505.x

Eski, I., Demir, B., Gürbüz, F., Kus, Z. A., Yilmaz, K. U., Uzun, M., & Ercisli, S. E. (2018). Design of neural network predictor for the physical properties of almond nuts. *Erwerbs-Obstbau*, *60*, 153–160. https://doi.org/10.1007/s10341-017-0349-3

Ghanbarian, D., Dastjerdi, M. B., & Torki-Harchegani, M. (2016). Mass transfer characteristics of bisporus mushroom (Agaricus bisporus) slices during convective hot air drying. *Heat and Mass Transfer*, *52*, 1081–1088. https://doi.org/10.1007/s00231-015-1629-9

Jafari, S. M., Ganje, M., Dehnad, D., & Ghanbari, V. (2016). Mathematical, fuzzy logic and artificial neural network modeling techniques to predict drying kinetics of onion. *Journal of Food Processing and Preservation*, *40*, 329–339. https://doi.org/10.1111/jfpp.12610

Jahanbakhshi, A. (2018). Determine some engineering properties of snake melon (Cucumis melo var. flexuosus). *Agricultural Engineering International: CIGR Journal*, *20*, 171–176.

Jahanbakhshi, A., Ghamari, B., & Heidarbeigi, K. (2017). Assessing acoustic emission in 1055I John Deere combine harvester using statistical and artificial intelligence methods. *International Journal of Vehicle Noise and Vibration*, *13*, 105–117. https://doi.org/10.1504/IJVNV.2017.087906

Jahanbakhshi, A., Rasooli Sharabiani, V., Heidarbeigi, K., Kaveh, M., & Taghinezhad, E. (2019). Evaluation of engineering properties for waste control of tomato during harvesting and postharvesting. *Food Science & Nutrition*, *7*, 1473–1481. https://doi.org/10.1002/fsn3.986

Jahanbakhshi, A., & Salehi, S. (2019). Processing watermelon waste using *Saccharomyces cerevisiae* yeast and the fermentation method for bioethanol production. *Journal of Food Process Engineering*, *42*(7), e13283. https://doi.org/10.1111/JFPE.13283

Karthikeyan, A. K., & Murugavelh, S. (2018). Thin layer drying kinetics and exergy analysis of turmeric (Curcuma longa) in a mixed mode forced convection solar tunnel dryer. *Renew Energy*, *128*, 305–312. https://doi.org/10.1016/j.renene.2018.05.061

Kaveh, M., Jahanbakhshi, A., Abbaspour-Gilandeh, Y., Taghinezhad, E., & Moghimi, M. B. F. (2018). The effect of ultrasound pre-treatment on quality, drying, and thermodynamic attributes of almond kernel under convective dryer using ANNs and ANFIS network. *Journal of Food Process Engineering*, *41*, e12868. https://doi.org/10.1111/jfpe.12868

Kaveh, M., Sharabiani, V. R., Amiri Chayjan, R., Taghinezhad, E., Abbaspour-Gilandeh, Y., & Golpour, I. (2018). Prediction of kinetic, effective moisture diffusivity and specific energy consumption for potato, garlic and cantaloupe drying under convective hot air dryer using neuro-fuzzy inference system and artificial neural networks. *Information Processing in Agriculture*, *5*, 372–387.

Kesavan, S., Arjunan, T. V., & Vijayan, S. (2019). Thermodynamic analysis of a triple-pass solar dryer for drying potato slices. *Journal of Thermal Analysis and Calorimetry*, *136*, 159–171. https://doi.org/10.1007/s10973-018-7747-0

Khanali, M., & Rafiee, S. (2014). Investigation of hydrodynamics, kinetics, energetic and exergetic aspects of fluidized bed drying of rough rice. *International Journal of Food Engineering*, *10*, 39–50. https://doi.org/10.1515/ijfe-2012-0116

Khoshnevisan, B., Rafiee, S., Omid, M., & Mousazadeh, H. (2014). Prediction of potato yield based on energy inputs using multi-layer adaptive neuro-fuzzy inference system. *Measurement*, *47*, 521–530. https://doi.org/10.1016/j.measurement.2013.09.020

Koukouch, A., Idlimam, A., Asbik, M., Sarh, B., Izrar, B., Bostyn, S., … Amine, A. (2017). Experimental determination of the effective moisture diffusivity and activation energy during convective solar drying of olive pomace waste. *Renewable Energy*, *101*, 565–574. https://doi.org/10.1016/j.renene.2016.09.006

Lingayat, A., Chandramohan, V. P., & Raju, V. R. K. (2018). Energy and exergy analysis on drying of banana using indirect type natural convection solar dryer. *Heat Transfer Engineering*, https://doi.org/10.1080/01457632.2018.1546804

Liu, Z. L., Bai, J. W., Wang, S. X., Meng, J. S., Wang, H., Yu, X. L., … Xiao, H. W. (2019). Prediction of energy and exergy of mushroom slices drying in hot air impingement dryer by artificial neural network. *Drying Technology*, https://doi.org/10.1080/07373937.2019.1607873

Majdi, H., Esfahania, J. A., & Mohebbi, M. (2019). Optimization of convective drying by response surface methodology. *Computer and Electronics in Agriculture*, *156*, 574–584. https://doi.org/10.1016/j.compag.2018.12.021

Mohammadi, I., Tabatabaekoloor, R., & Motevali, A. (2019). Effect of air recirculation and heat pump on mass transfer and energy parameters in drying of kiwifruit slices. *Energy*, *170*, 149–158. https://doi.org/10.1016/j.energy.2018.12.099

Motevali, A., Jafari, H., & Hashemi, S. J. (2018). Effect of IR intensity and air temperature on exergy and energy at hybrid infrared- hot air dryer. *Chemical Industry and Chemical Engineering Quarterly*, *24*, 31–42. https://doi.org/10.2298/CICEQ170123015M

Motevali, A., & Minaei, S. (2012). Effects of microwave pretreatment on the energy and exergy utilization in thin-layer drying of sour pomegranate arils. *Chemical Industry and Chemical Engineering Quarterly*, *18*, 63–72. https://doi.org/10.2298/CICEQ110702047M

Motevali, A., Minaei, S., Banakar, A., Ghobadian, B., & Khoshtaghaza, M. H. (2014). Comparison of energy parameters in various dryers. *Energy Conversion and Management*, *87*, 711–725. https://doi.org/10.1016/j.enconman.2014.07.012

Motevali, A., & Tabatabaei, S. R. (2017). A comparison between pollutants and greenhouse gas emissions from operation of different dryers based on energy consumption of power plants. *Journal of Cleaner Production*, *154*, 445–461. https://doi.org/10.1016/j.jclepro.2017.03.219

Movagharnejad, K., & Nikzad, M. (2007). Modeling of tomato drying using artificial neural network. *Computer and Electronics in Agriculture*, *59*, 78–85. https://doi.org/10.1016/j.compag.2007.05.003

Nazghelichi, T., Aghbashlo, M., Kianmehr, M. H., & Omid, M. (2011). Prediction of energy and exergy of carrot cubes in a fluidized bed dryer by artificial neural networks. *Drying Technology*, *29*, 295–307. https://doi.org/10.1080/07373937.2010.494237

Nazghelichi, T., Kianmehr, M. H., & Aghbashlo, M. (2010). Thermodynamic analysis of fluidized bed drying of carrot cubes. *Energy*, *35*, 4679–4684. https://doi.org/10.1016/j.energy.2010.09.036

Nikbakht, A. M., Motevali, A., & Minaei, S. (2014). Energy and exergy investigation of microwave assisted thin-layer drying of pomegranate arils using artificial neural networks and response surface methodology. *Journal of the Saudi Society of Agricultural Sciences*, *13*, 81–91. https://doi.org/10.1016/j.jssas.2013.01.005

Omari, A., Behroozi-Khazaei, N., & Sharifian, F. (2018). Drying kinetic and artificial neural network modeling of mushroom drying process in microwave-hot air dryer. *Journal of Food Process Engineering*, *41*, e12849. https://doi.org/10.1111/jfpe.12849

Onwude, D. I., Hashim, N., Abdan, K., Janius, R., & Chen, G. (2019). The effectiveness of combined infrared and hot-air drying strategies for sweet potato. *Journal of Food Engineering*, *241*, 75–87. https://doi.org/10.1016/j.jfoodeng.2018.08.008

Rad, S. J., Kaveh, M., Sharabiani, V. R., & Taghinezhad, E. (2018). Fuzzy logic, artificial neural network and mathematical model for prediction of white mulberry drying kinetics. *Heat and Mass Transfer*, *54*, 3361–3374. https://doi.org/10.1007/s00231-018-2377-4

Ranjbaran, M., & Zare, D. (2013). Simulation of energetic- and exergetic performance of microwave-assisted fluidized bed drying of soybeans. *Energy*, *15*, 484–493. https://doi.org/10.1016/j.energy.2013.06.057

Roknul Azam, S. M., Zhang, M., Law, C. L., & Mujumdar, A. S. (2019). Effects of drying methods on quality attributes of peach (Prunus persica) leather. *Drying Technology*, *37*, 341–351.

Sahin, M., & Doymaz, I. (2017). Estimation of cauliflower mass transfer parameters during convective drying. *Heat and Mass Transfer*, *53*, 507–517. https://doi.org/10.1007/s00231-016-1835-0

Samimi-Akhijahani, H., & Arabhosseini, A. (2018). Accelerating drying process of tomato slices in a PV-assisted solar dryer using a sun tracking system. *Renewable Energy*, *123*, 428–438. https://doi.org/10.1016/j.renene.2018.02.056

Savari, M., Moghaddam, A. H., Amiri, A., Shanbedi, M., & Ayub, M. N. B. (2017). Comprehensive heat transfer correlation for water/ethylene glycol-based graphene (nitrogen-doped graphene) nanofluids derived by artificial neural network (ANN) and adaptive neuro-fuzzy inference system (ANFIS). *Heat and Mass Transfer*, *53*, 3073–3083. https://doi.org/10.1007/s00231-017-2047-y

Sehrawat, R., Nema, P. K., & Kaur, B. P. (2018). Quality evaluation and drying characteristics of mango cubes dried using lowpressure superheated steam, vacuum and hot air drying methods. *LWT-Food Science and Technology*, *92*, 548–555. https://doi.org/10.1016/j.lwt.2018.03.012

Şevik, S., Aktaş, M., Dolgun, E. C., Arslan, E., & Tuncer, A. D. (2019). Performance analysis of solar and solar-infrared dryer of mint and apple slices using energy-exergy methodology. *Solar Energy*, *180*, 537–549. https://doi.org/10.1016/j.solener.2019.01.049

Shekarchizadeh, H., Tikani, R., & Kadivar, M. (2014). Optimization of cocoa butter analog synthesis variables using neural networks and

genetic algorithm. *Journal of Food Science and Technology*, *51*, 2099–2105. https://doi.org/10.1007/s13197-012-0695-y

Shende, D., & Datta, A. K. (2019). Refractance window drying of fruits and vegetables: A review. *Journal of the Science of Food and Agriculture*, *99*, 1449–1456. https://doi.org/10.1002/jsfa.9356

Sun, Q., Zhang, M., & Mujumdar, A. S. (2019). Recent developments of artificial intelligence in drying of fresh food: A review. *Critical Reviews in Food Science and Nutrition*, *59*, 2258–2275. https://doi.org/10.1080/10408398.2018.1446900

Surendhar, A., Sivasubramanian, V., Vidhyeswari, D., & Deepanraj, B. (2019). Energy and exergy analysis, drying kinetics, modeling and quality parameters of microwave-dried turmeric slices. *Journal of Thermal Analysis and Calorimetry*, *136*, 185–197. https://doi.org/10.1007/s10973-018-7791-9

Taheri-Garavand, A., Karimi, F., Karimi, M., Lotfi, V., & Khoobbakht, G. (2018). Hybrid response surface methodology–artificial neural network optimization of drying process of banana slices in a forced convective dryer. *Food Science and Technology International*, *24*, 277–291. https://doi.org/10.1177/1082013217747712

Torki-Harchegani, M., Ghanbarian, D., Pirbalouti, A. G., & Sadeghi, M. (2016). Dehydration behaviour, mathematical modelling, energy efficiency and essential oil yield of peppermint leaves undergoing microwave and hot air treatments. *Renewable and Sustainable Energy Reviews*, *58*, 407–418. https://doi.org/10.1016/j.rser.2015.12.078

Yogendrasasidhar, D., & Setty, Y. P. (2018). Drying kinetics, exergy and energy analyses of Kodo millet grains and Fenugreek seeds using wall heated fluidized bed dryer. *Energy*, *151*, 799–811. https://doi.org/10.1016/j.energy.2018.03.089

Ziaforoughi, A., Yousefi, A. R., & Razavi, S. M. A. (2016). A comparative modeling study of quince infrared drying and evaluation of quality parameters. *International Journal of Food Engineering*, *12*, 901–910. https://doi.org/10.1515/ijfe-2016-0074

Zohrabi, S., Seiiedlou, S. S., Aghbashlo, M., Scaar, H., & Mellmann, J. (2019). Enhancing the exergetic performance of a pilot-scale convective dryer by exhaust air recirculation. *Drying Technology*, https://doi.org/10.1080/07373937.2019.1587617

How to cite this article: Abbaspour-Gilandeh Y, Jahanbakhshi A, Kaveh M. Prediction kinetic, energy and exergy of quince under hot air dryer using ANNs and ANFIS. *Food Sci Nutr.* 2020;8:594–611. https://doi.org/10.1002/fsn3.1347